

A NEW LIDAR-BASED APPROACH FOR POLES AND DISTRIBUTION LINES DETECTION AND MODELLING

Mohamed Gaha¹, Wael Jaafar², Jed Fakhfekh³, Guillaume Houle¹,
Jihene Ben Abderrazak³ and Michel Bourgeois¹

¹Hydro-Quebec Research Institute, Quebec, Canada

²Carleton University, Ontario, Canada

³ESPRIT Engineering School, Tunis, Tunisia

ABSTRACT

Vegetation is the major cause of overhead power line failures. According to a recent Hydro-Quebec analysis, more than 60% of the power outages are related to vegetation. Specifically, when branches/trees nearby the distribution network interact with extreme weather conditions, e.g., melting snow and heavy rain, they may bend and cause power outages. To ensure the reliability of our distribution network, millions of dollars are yearly spent for pruning trees and trimming branches. Aiming to reduce these costs, we recently adopted a new approach based on light detection and ranging (LiDAR) data. Indeed, we scanned 150 km of Hydro-Quebec's network using a mobile LiDAR system. Through data analysis, we target automatic detection of hot spots, i.e., locations of threatening branches to distribution lines. However, such an operation cannot be accurately completed without a prior efficient detection of poles and lines locations, even for incomplete or missing LiDAR data. Hence, we propose here a low-complex and robust method for poles/distribution lines detection and lines modelling. Through customized filtering and detection, we efficiently detect poles and distribution lines with high accuracy and recall. Indeed, poles are detected with an accuracy of 94.5% and a recall of 89.7%, while lines are detected with an accuracy of 84% and a recall of 98.9%. Finally, our approach reconstructs power lines with a distance deviation from the real ones below 20 cm, in 89% of the cases. Such accuracy is required to automatically evaluate the closeness of vegetation to distribution lines and prevent power outages.

KEYWORDS

Mobile LiDAR, power lines, distribution lines detection, poles detection, distribution lines modelling.

1. INTRODUCTION

Distribution overhead power lines are often victims of outages caused by vegetation. According to a recent study by Hydro-Quebec, vegetation, specifically tree branches, are the cause of more than 60% of the power outages in the province of Quebec, Canada [1]. Such phenomenon is mainly triggered by extreme weather conditions, such as melting snow, gust, and heavy rain, which force the tree branches to bend and hit the power lines causing outages. To improve the reliability of the distribution network, power utilities spend millions of dollars yearly to trim and cut vegetation and to secure the space around the power lines. At Hydro-Quebec, to identify the lines that require vegetation pruning interventions, past historical data on vegetation outages are analyzed, then processed to identify the worst lines requiring an immediate intervention. Subsequently, the identified lines information is transferred to the "Department of Vegetation

Management", which evaluates the intervention tasks. A forester is then sent to inspect visually each line, identify the exact locations of the trees to be pruned, and evaluate the workload. This process is complex since it involves several resources and expertise, in addition to a high coordination level between different departments.

Aiming to optimize these processes, recently we decided, at Hydro-Quebec, to adopt a novel colored light detection and ranging (LiDAR) based approach. Indeed, using a mobile LiDAR system (MLS) mounted over a motorized vehicle; we scanned 150 km of our distribution network. The MLS is a new scanning technique that uses a dense point cloud laser to measure distances between the laser source and any object in the surrounding three-dimensional (3D) space, i.e., according to the x , y and z planes.

The MLS technique is becoming popular as it provides a high-level of details and it returns valuable information on the vegetation and the asset's location. Also, its acquisition costs have significantly dropped over the last ten years, thus making it an interesting alternative to the airborne laser scanning system [2].

The objective of using the MLS point cloud is to automatically detect, as a forester, "The Hot Spot", i.e., locations where branches are close to the distribution network. In this paper, we present a novel algorithm that accurately detects the location of power poles and distribution lines. The detection of the power lines is possible even using incomplete or highly obstructed LiDAR data. Thus, any point cloud that is close to the lines are identified as being vegetation. Later, this information will be used as an insight for vegetation workload.

1.1. Related Work

Power line mapping using an airborne laser scanning (ALS) system was studied in several works [3]-[5]. In many studies the intensity of the laser beam reflection or the height of the pulses are used to locate the lines and the transmission pylon. Such techniques are adequate with LiDAR-based ALS due to the direct line-of-sight between the lines and aircraft above them. However, these specific techniques may not be suitable for the distribution network due to the wire diameters of the low voltage network [2]. In contrast, the number of LiDAR points per square metre collected by the ALS is between half and a tenth of that collected by the MLS, which makes the detection of low-voltage lines very approximate.

Power line detection using MLS data was initially investigated in [6]-[8]. In [9], Guan *et al.* presented a method for extracting power transmission lines and pylons from MLS data. After removing the ground, they extract the power transmission lines according to the height, spatial density, shape, and points' density criteria. A 3D power line was modelled through its projection as a horizontal line in the (x, y) plane and as a two-dimensional (2D) catenary curve in the (x, z) plane. This projection procedure simplifies the calculation of the 3D catenary curve parameters. Then, the detected lines from the top-down view are clustered and used to accurately detect the power poles. However, this method requires high density point clouds for accurate power lines detection, which would be inefficient for power lines obstructed by vegetation or with low points' density. The overhead power lines with low point density affect the accuracy of the proposed method.

Yadav and Chousalkar proposed in [10] a different power lines extraction method. First, the horizontal segments containing power lines are filtered based on the distance between the ground and the points' heights. Then, a 2D density approach is used to remove trees and buildings. Finally, the Hough-Transform is applied to extract the lines, and missing lines portions are reconstructed using a second-order curve fitting technique. They reported a reconstruction

precision rate of 84% in an urban site and of 99% in a rural environment. Although their method works well in partially occluded environments, it is still limited for areas heavily occluded by vegetation.

Recently, the authors of [2] combined several techniques to improve the detection capability. After filtering out the ground and buildings, they extracted horizontal lines from the remaining LiDAR point clouds using a modified version of the well-known random sample consensus (RANSAC) algorithm. Subsequently, the extracted horizontal line candidates were classified based on several criteria, i.e., the vertical distance above the ground, the points' density, and the linearity measure. Next, the authors proceeded with the poles' detection. The main reason is to retrieve less false positive pole candidates based on the detected power line data. Specifically, poles closer than 2m to the extracted power lines and where the angle between the lines and the poles is approximately 45° were detected and retrieved. However, this study did not approximate the power lines to compensate for the missing LiDAR points. Moreover, if many power lines LiDAR points are missing or are occluded by the vegetation, the lines and poles detection procedure would fail.

1.2. Contributions

To tackle the limitations of state-of-art works, we propose in this paper an efficient and powerful approach for poles and power lines detection and extraction using MLS acquired data. Then we reconstruct overhead model power lines.

The contributions of our work can be summarized as follows:

1. First, unlike the previous works, we start by detecting the power poles before power lines. By doing so, we significantly reduce the system's complexity since power lines detection becomes limited into small volumes bounded by subsequent pairs of poles.
2. Second, through our proposed colour-based filtering, the accuracy of our line detection method is improved and operates efficiently even in heavily occluded areas by vegetation.
3. Finally, using a 3D parabola equations system, we rapidly reconstruct the 3D power lines shapes with a very high precision rate.

2. PROPOSED POLES AND DISTRIBUTION LINES DETECTION APPROACH

In this study, we develop a new approach for poles and power lines detection, whose steps are summarized in Figure 1 and are detailed below. All the described steps were developed with the C++ point cloud library (PCL) [11].

For the sake of clarity, we illustrate the following steps using a sample file of LiDAR data selected from the Hydro-Quebec dataset. The sample file contains the LiDAR point cloud of a rural single-phase distribution lines corridor, as illustrated in Figure 2. The point cloud contains many objects within the area, including the road, the vegetation, the power poles, and the power lines.

2.1. Power Poles Detection

Prior to the detection of poles, we reduce the search space within the LiDAR point cloud. To do so, we start by removing the ground surface points. This is executed using the "Progressive Morphological Filter", proposed by Zhang *et al.* in [12]. A simple implementation of this filter is

available in the PCL library. Consequently, the LiDAR point cloud is reduced, on average, by 40%.

Next, we cluster the 3D points based on a Euclidean distance rule, applied on the points' locations, and using a point cloud density function. Then, clusters are filtered according to their size, width, and height. Figure 3 shows the obtained clusters from the original track. We notice that it contains 9 distinct clusters including 7 poles.

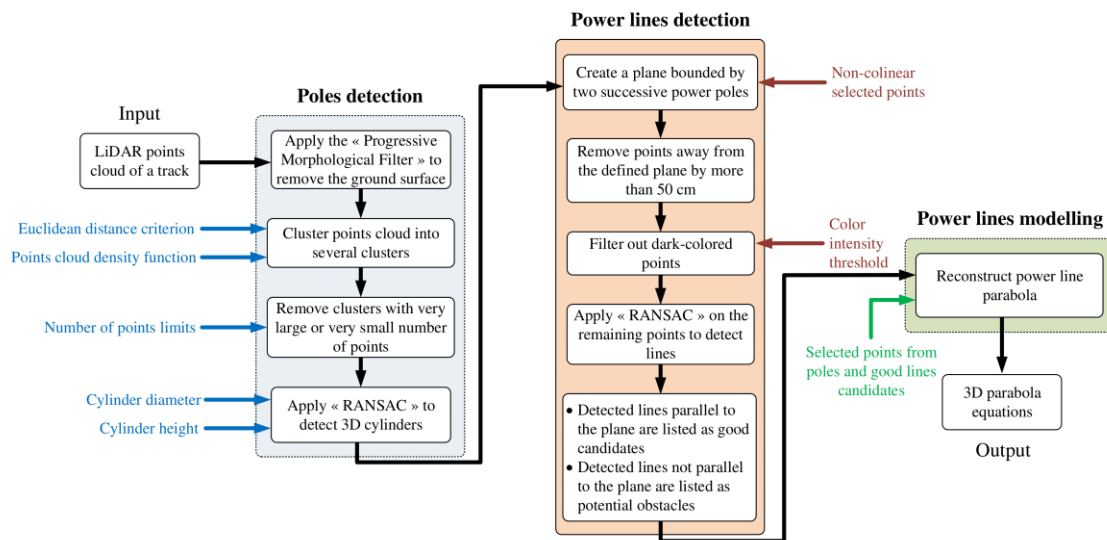


Figure 1: Flowchart of the proposed poles and power lines detection approach

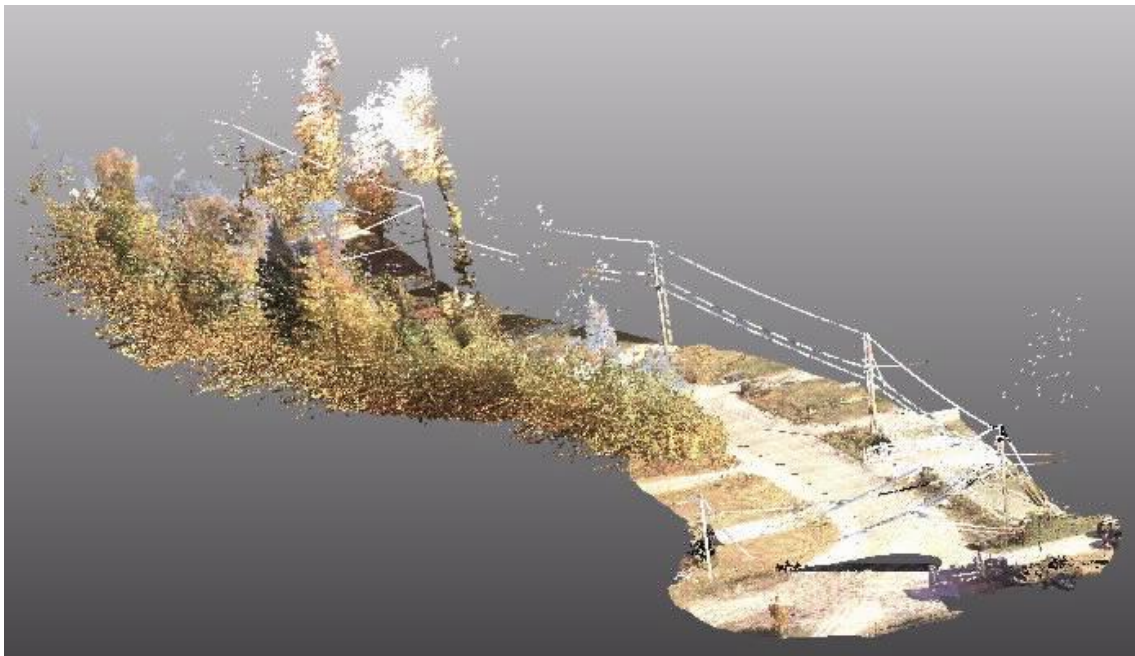


Figure 2: A sample of collected mobile LiDAR data along a distribution power lines in a rural area

Finally, for each cluster, we use the RANSAC algorithm to detect 3D cylinder shapes from point clouds [13]. Each detected cylinder must be parallel to the z -axis with a maximal deviation of 15°

and should not exceed a diameter of 60 cm with a maximum height of 11.5 m. Furthermore, the number of points composing a pole must be more than 3k LiDAR points. When several collocated cylinders are detected within the same point cloud cluster, it is inferred that these cylinders belong to the same pole. The accuracy of our algorithm is summarized in the next section.

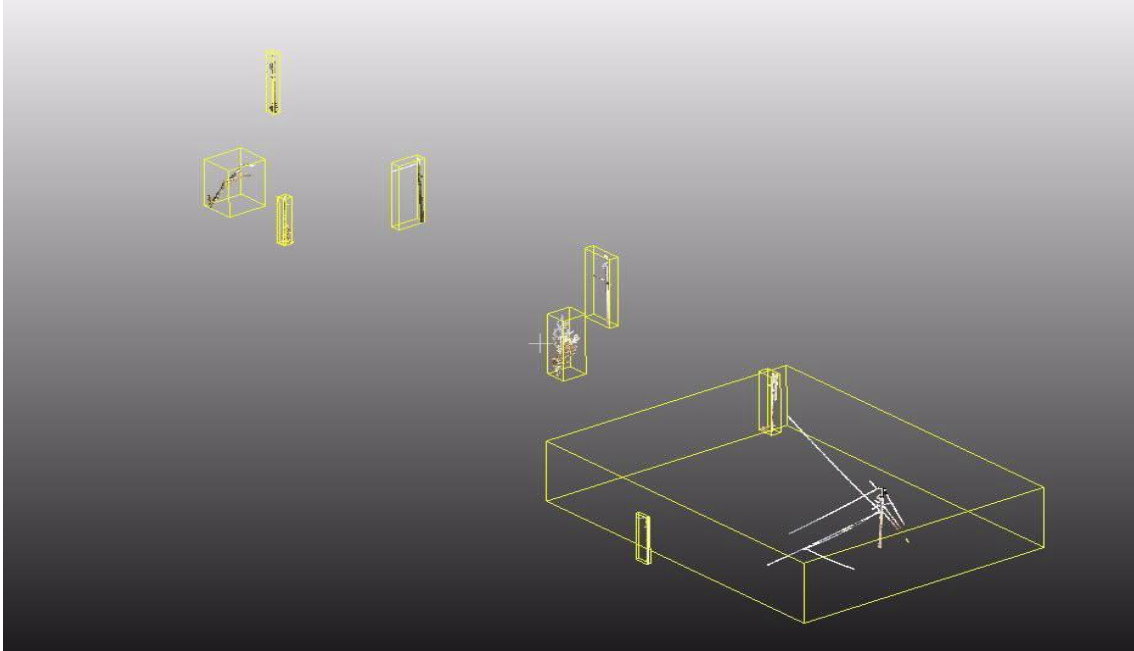


Figure 3: Clustering the point cloud

2.2. Power Lines Detection

Once the poles are detected, we create a plane bounded by two successive power poles. This plane offers valuable information to detect power lines. First, it tremendously reduces the amount of data to process since power lines are necessarily close to the defined plane. Second, all the power lines are inevitably parallel to this plane. When a line is not parallel to our plane, it is inferred that it is part of the vegetation. Later, this information will be used as an insight for vegetation workload.

To create a plane, at least three non-collinear points are required. Since single-phase distribution lines are typically attached at the top of poles, we select the first two points of the plane from the top of two consecutive poles. Then, the third point is selected from the bottom of one of the poles. In the 3D space, a plane P is characterized by the following equation:

$$P : ax + by + cz + d = 0, \quad (1)$$

where the parameters a , b , c , and d are real numbers and (x, y, z) are the coordinates of a point belonging to the plane.

Subsequently, we calculate the distances between any points and the defined plane. Assume that a point O has coordinates (x_0, y_0, z_0) , then the perpendicular distance from the plane P can be defined by

$$d(O,P) = |ax_0 + by_0 + cz_0 + d| / \sqrt{(a^2+b^2+c^2)}, \quad (2)$$

where $|\cdot|$ is the absolute value function.

In the following step, we filter out all points having $d(O,P) > 50$ cm, as illustrated in Figure 4. This operation significantly reduces the number of power lines candidate points, compared to the original track. Hence, searching lines using the RANSAC algorithm becomes very efficient and returns good candidates with a higher probability of being overhead power lines [14].



Figure 4: Filtered point cloud close to the planes delimited by the poles

Indeed, the RANSAC algorithm is very efficient when the number of points to process is low. It starts by randomly selecting points and calculates the number of inliers and outliers according to a mathematical model, e.g., it selects two points to draw a 3D line and finds inliers and outliers within the defined line. This process is iteratively repeated until the highest number of inliers is obtained.

In our approach, we propose to classify all the lines detected by RANSAC as follows. When a line is parallel to P , it is classified as a power line candidate; otherwise, it is listed as a potential branch or vegetation. This classification eliminates the false positive candidates, i.e., the detected lines falsely seen as candidates of real power lines.

To classify a RANSAC detected line, which is delimited by extremity points $O_1(x_1, y_1, z_1)$ and $O_2(x_2, y_2, z_2)$, as a good candidate or not, we check if it is parallel to plane P through the following condition:

$$a(x_2 - x_1) + b(y_2 - y_1) + c(z_2 - z_1) = 0. \quad (3)$$

Remark. Note that the efficiency of RANSAC in this step is highly dependent on the quality of the reduced point cloud. If relying only on the 50 cm distance condition to filter points around the defined plane, there is a high probability that several non-relevant points, e.g., vegetation and other obstacles, would be kept within the area of interest, particularly when heavily occluded by

vegetation. The presence of such points may distort the line detection procedure as RANSAC is forced to maximize the number of inlier points, while including them as potential line points.

In order to tackle this limitation, we propose for the first-time colour-based filtering. Indeed, we noticed that typically power line points have a brighter colour than other objects in the environment. Hence, we apply a filter that removes dark-coloured points after the distance-based filtering. This process is conducted with respect to a selected colour intensity threshold. Practically, we only keep the following red-green-blue (RGB) values:

$$RGB = (185 \pm 75, 185 \pm 75, 185 \pm 75). \quad (4)$$

Although this approach may sacrifice several relevant points, it doesn't affect RANSAC's performance due to the latter's robustness using a low number of points.

2.3. Power Lines Modelling

The power lines recorded by the MLS are sometime incomplete or obstructed. Indeed, depending on the power line location with respect to the LiDAR scanner's position, on the height and diameter of the line and on the extent of the vegetation's encroachment, important sections of the line are frequently missing or invisible. In this situation, it becomes mandatory to accurately model those missing line parts and fully exploit them to recover the absent line sections and correctly evaluate the encroachment of the tree branches along the power line.

For the single-phase distribution network, we reconstruct the 3D parabola shape of a power line by strategically selecting three points. The first and second points, denoted by $O_1(x_1, y_1, z_1)$ and $O_2(x_2, y_2, z_2)$, are selected from the top of two consecutive poles, while the third point, $O_3(x_3, y_3, z_3)$, is taken from the detected lines between the same poles. The 3D parabola can be characterized by two equations as follows. By projecting the parabola on the (x, y) horizontal plane, it can be seen as a line with equation $L_1 : y = a_1x + b_1$ whereas, when projected on the (x, z) vertical plane, it is modelled as a 2D parabola with equation $L_2 : z = a_2x^2 + b_2x + c_2$.

By substituting the coordinates of the selected points into L_1 and L_2 , respectively, two systems of equations are obtained and solved to determine the parameters. The latter can be given by:

$$a_1 = (y_2 - y_1) / (x_2 - x_1) \quad (5a)$$

$$b_1 = y_1 - a_1 x_1 \quad (5b)$$

$$a_2 = [y_3(x_2 - x_1) + y_2(x_1 - x_3) + y_1(x_3 - x_2)] / [(y_1 - y_2)(y_1 - y_3)(y_2 - y_3)] \quad (5c)$$

$$b_2 = [(y_3)^2(x_2 - x_1) + (y_2)^2(x_1 - x_3) + (y_1)^2(x_3 - x_2)] / [(y_1 - y_2)(y_1 - y_3)(y_2 - y_3)] \quad (5d)$$

$$c_2 = z_1 - a_2(x_1)^2 - b_2x_1. \quad (5e)$$

Figure 5 shows the 3D parabola curves built from the detected poles and lines. As it can be seen, it efficiently recovers the line's missing points and returns, with high accuracy, the exact location of the single-phase power lines.

3. CASE STUDY AND RESULTS

3.1. Case Study

3.1.1. MLS Setup and Datasets

The 3D mobile LiDAR point cloud data was collected with the Leica Pegasus mobile mapping system using seven 4 Megapixels cameras and a ZF 9012 sensor, having the accuracy of 9 mm at 50 m. Data acquisition was realized in Mont-Laurier, Quebec, in October 2019, and the linear surveyed distance was 150 km long and included both urban and rural sections.

For this work, we used two datasets of LiDAR points. The first, used for the approach's development and fine-tuning, contains subsections of 68 poles. The second, used for the approach's testing and validation, possesses subsections of 98 poles. Both sets of data are Hydro-Quebec's property and cannot be publicly shared.

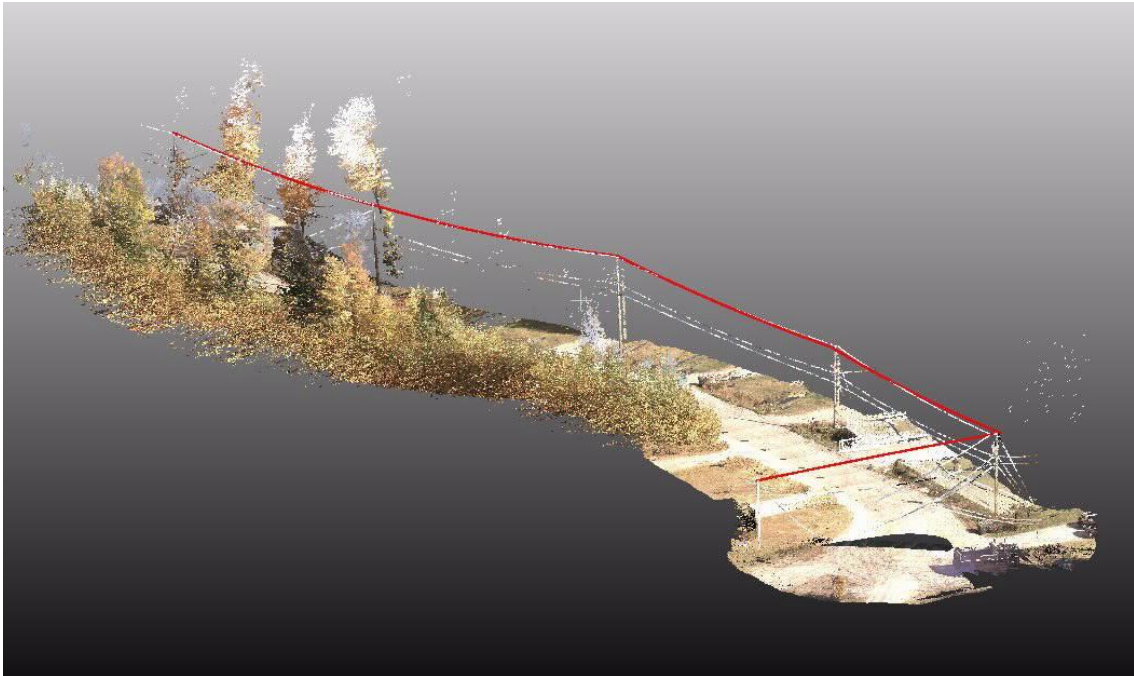


Figure 5: Power lines modelling using 3D parabola equation (in red)

3.1.2. Poles Detection Setup

During the clustering step, we keep all the clusters that have a point cloud size between 3k and 100k points (i.e., the “Point cloud density function” and “Number of points limits” criteria). The height of the cluster should not exceed 11.5 m and the width should be less than 2 m. With this technique, we only keep potentially good candidates.

For each cluster, we execute the RANSAC 3D cylinder detection algorithm. The diameter and the height of the cylinder should not exceed 60 cm and 11.5 m, respectively (i.e., “Cylinder height” and “Cylinder diameter” criteria), while its orientation is below 15° , along the Z-axis.

3.1.3. Power Lines Detection and Modelling Setup

After the poles' detection step, we link the poles two-by-two according to their Euclidean distances that should be more than 20 m and less than 65 m. A plane can be created between two linked poles, and points that are within a distance up to 50 cm from the plane, with respect to the RGB colouring criterion (4), are extracted. The obtained region of interest is then analyzed to detect sticks (i.e., 3D lines) that have a radius ranging between 1 cm and 3 cm, and a minimum point cloud density of 40 LiDAR points. When the sticks are parallel to the plane and have the appropriate length and size, they are selected to mathematically model a parabola between two poles.

All the modelled parabolas are ranked according to their proximity with the previously detected sticks. The distance between the sticks and the parabola is incrementally processed and should not exceed 20 cm.

Finally, the parabola with the highest number of LiDAR sticks points is selected as the best one representing the overhead power line.

3.2. Results

In Table 1, we present the pole detection performances in terms of the number of true positive poles (i.e., real detected poles), the number of false positive poles, the accuracy, and the recall, for different values of the RANSAC minimum height parameter.

Table 1: Poles detection accuracy and recall for different RANSAC poles height

Min. pole height	No. of true positive poles	No. of false positive poles	Accuracy	Recall
7.5 m	154	26	92.7 %	85.5 %
6 m	157	18	94.5 %	89.7 %

As it can be seen, an accuracy of 92.7% and a recall of 85.5% are obtained for the minimum pole height of 7.5 m, while the accuracy and recall increase to 94.5% and 89.7%, respectively, for the minimum pole height of 6 m. This is expected since lowering the minimum pole height parameter to 6 m allows considering more relevant poles cloud points in the RANSAC algorithm. However, going below 6 m would consider irrelevant cloud points causing a high number of false positives. The obtained results are promising; however, they require extensive probing to ensure that the minimum height parameter value of 6 m is valid for any recorded point cloud cluster. Also, depending on the LIDAR hardware tuning and speed of the vehicle, the LIDAR points density may vary, thus affecting our algorithm's performances in terms of accuracy and recall. Hence, prior to any LIDAR recording, we strongly recommend using the same hardware settings to have reproducible results.

For power lines detection, we reached in our experiments the accuracy of 84%, given minimum pole height of 6 m. Such a high result is achieved due to the efficient poles detection and LiDAR data filtering steps prior to RANSAC based lines detection. Also, an outstanding line detection recall of 98.9% is realized. This result is mainly since all sticks candidates are representative of the final solution. Moreover, highly obstructed lines were correctly detected, thus making lines detection very efficient compared to state-of-art methods.

In order to emphasize the performance of our lines modelling approach, we illustrate in Figure 6 the distribution of the distance gap between the real and reconstructed power lines, given three different reconstruction methods. The latter differ in the selection of the poles' points $O_1(x_1, y_1, z_1)$ and $O_2(x_2, y_2, z_2)$ when modelling the power lines with 3D parabolas. In each pole, the z_i coordinate of point O_i ($i = 1, 2$) is selected as the highest point of the pole. However, optimally selecting (x_i, y_i) coordinates is not straight-forward. Indeed, the extracted cylinder that represents the pole is not perfectly cylindrical and can contain cloud points of vegetation, wires, signs, or any equipment attached to the pole.

For the sake of simplicity, we developed three methods to adequately select the (x_i, y_i) coordinates ($i = 1, 2$). Specifically, "Method 1" selects the averaged (x, y) location on the upper half subsection of the pole, "Method 2" takes the averaged location on the lower half subsection of the pole, whereas "Method 3" selects the average (x, y) location on the central subsection of the pole. In Figure 6, both "Method 1" and "Method 3" present the best performances with a preference to "Method 1". Indeed, the obtained distance gap between the real and reconstructed lines is less than 10 cm and 20 cm in 66% and 89% of the cases, respectively. In contrast, "Method 2" has the worst performance, with a gap of 20 cm or less in 78% of the cases. We conclude that the selection of the 3D parabola reconstructing points' locations is crucial for

accuracy. Hence, a precise 3D parabola model of power lines would allow accurately estimating the vegetation closeness and thus evaluating the risk of outages.

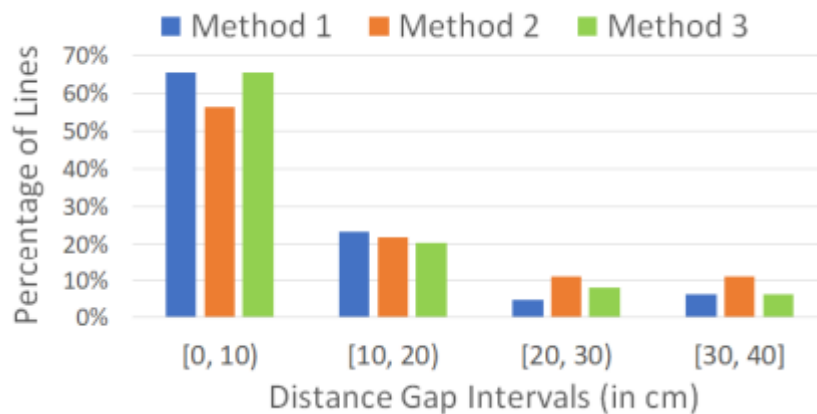


Figure 6: Distribution of distance gap between real and reconstructed overhead power lines for three modelling methods

4. LIMITATIONS AND FUTURE WORK

As demonstrated in the previous section, our approach is effective in detecting poles and power lines. However, it is limited to single-phase lines, and still experiences some issues in fully occluded environments. In any case, we believe that our approach's accuracy can be further improved using the following rules.

First, more selective filtering techniques should be applied. For instance, we noticed that relevant LiDAR data is located at distances less than 7.5 m from the MLS detector. Indeed, the poles are usually close to the road and within a clear view from the MLS. Hence, only this data should be processed and analyzed. Second, the poles are typically located within one side only of the road. Thus, our algorithm can be used on the right or left side of the motorized LiDAR. Once the poles and cables are detected on one side of the road, it can skip processing remaining data on the

opposite side. To do so, an indicator can be used to guide the detection algorithm and can help decide which side of the road to process first. This simple rule reduces the algorithm's processing time by at least 25%.

Finally, recent MLS systems have, in addition to the laser scanner, six digital cameras recording 360° images. These 2D pictures are recorded along the LiDAR scanner data at different timestamps.

Since deep learning neural networks are highly efficient in detecting objects in 2D images [15], it becomes interesting to integrate this feature into our approach to improve the LiDAR data segmentation process. Indeed, combining several images of the same object at different timestamps allows building a corresponding frustum in the 3D LiDAR space [16], [17]. The latter reduces the original LiDAR space into a small 3D box. Thus, object detection and segmentation of the LiDAR data become a simple clustering process. We conducted preliminary experiments on this approach, and we had promising results.

In order to generalize our algorithm's application beyond single-phase line detection, e.g., to three-phase power lines detection, additional steps have to be introduced into our approach. For instance, since the horizontal distances between the three-phase lines are known, it is easy to mathematically split the 3D box between two poles (steps 1-2 in "Power lines detection", Figure 1) into three adjacent and parallel planes and their corresponding new 3D boxes. In each new plane, a line parabola modelling the phase is then built. Hence, generalization to three-phase line detection can be processed with minimum change.

5. CONCLUSION

In this paper, we proposed a new method to recognize and model the overhead power lines. We detected with high accuracy poles and power lines, even in heavily occluded environments.

To do so, we proposed an original approach that relies on multiple filters to parse the point cloud data, detects at first the poles, detects segments of the lines in second, and finally model the distribution lines with precise parabolas. The key idea is to use the locations of the detected poles to guide the lines detection and extraction process through simple geometrical operations.

Through our approach, we were able to detect power poles with accuracy up to 94.5%, while power lines were detected with the best accuracy of 84% and recall of 98.9%. Also, the reconstructed distribution lines, using the 3D parabolas, have a maximum deviation of 20 cm from the LiDAR data in 89% of the cases, which is very accurate for our application.

As a future work, further refinements will be applied to generalize our algorithm to detect three-phase power lines. Also, since 2D poles' images can be automatically segmented using convolutional neural networks, we start using image segmentation to automatically extract frustum. First experiments revealed that the power poles cloud detection within a frustum is highly accurate and the number of false positive is close to zero. With these promising results, our next step is to start detecting all the poles and the distribution lines for the recorded Lidar track of 150 km including both urban and rural sections.

REFERENCES

- [1] Hydro-Québec. (2019) Setting new sights with our clean energy. Annual Report. [Online] <https://www.hydroquebec.com/data/documents-donnees/pdf/annual-report-2019-hydro-quebec.pdf>
- [2] M. Lehtomaki, A. Kukko, L. Matikainen, J. Hyypä, H. Kaartinen, and A. Jaakkola, "Power line mapping technique using all-terrain mobile laser scanning," *Automation in Construction*, vol. 105, p. 102802, Sep. 2019.
- [3] M. Ax, S. Thamke, L. Kuhnert, and K. D. Kuhnert, "UAV based laser measurement for vegetation control at high-voltage transmission lines," in *Adv. Power and Elec. Engineer., ser. Adv. Mater. Res.*, vol. 614, 22013, pp. 1147–1152.
- [4] A. Jaakkola, J. Hyypä, A. Kukko, X. Yu, H. Kaartinen, M. Lehtomaki, and Y. Lin, "A low-cost multi-sensoral mobile mapping system and its feasibility for tree measurements," *ISPRS J. Photogramm. Remote Sens.*, vol. 65, no. 6, pp. 514–522, Nov. 2010.
- [5] A. Jaakkola, J. Hyypä, X. Yu, A. Kukko, H. Kaartinen, X. Liang, H. Hyypä, and Y. Wang, "Autonomous collection of forest field reference — The outlook and a first step with UAV laser scanning," *Remote Sens.*, vol. 9, no. 8, p. 785, Jul. 2017.
- [6] A. Kukko, C.-O. Andrei, V.-M. Salminen, H. Kaartinen, Y. Chen, P. Ronnholm, R. Chen, H. Haggren, I. Kosonen, and K. Capek, "Road environment mapping system of the Finnish geodetic institute- FGI roamer," in *Proc. of ISPR Wrkshp.*, 2007, pp. 241–247.
- [7] G. Petrie, "An introduction to the technology: Mobile mapping systems," *Geoinformatics*, vol. 13, no. 1, pp. 32–43, Jan./Feb. 2010.
- [8] I. Puente, H. Gonzalez-Jorge, J. Martinez-Sanchez, and P. Arias, "Review of mobile mapping and surveying technologies," *Measurement*, vol. 46, no. 7, pp. 2127–2145, Aug. 2013.
- [9] H. Guan, Y. Yu, J. Li, Z. Ji, and Q. Zhang, "Extraction of power-transmission lines from vehicle-borne LiDAR data," *Int. J. Remote Sens.*, vol. 37, no. 1, pp. 229–247, Jan. 2016.
- [10] M. Yadav and C. G. Chousalkar, "Extraction of power lines using mobile LiDAR data of roadway environment," *Remote Sensing Applications: Society and Environment*, vol. 8, pp. 258 – 265, Nov. 2017.
- [11] R. B. Rusu and S. Cousins, "3D is here: Point Cloud Library (PCL)," in *IEEE Int. Conf. Robot. Autom. (ICRA)*, Shanghai, China, May 9-13 2011.
- [12] K. Zhang, S.-C. Chen, D. Whitman, M.-L. Shyu, J. Yan, and C. Zhang, "A progressive morphological filter for removing nonground measurements from airborne LIDAR data," *IEEE Trans. Geosci. Remote Sensing*, vol. 41, no. 4, pp. 872–882, Apr. 2003.
- [13] T. Chaperon and F. Goulette, "Extracting cylinders in full 3D data using a random sampling method and the Gaussian image." in *Proc. Vision Model. Visualization Conf. (VMVC)*. Aka GmbH, 2001, pp. 35–42.
- [14] M. A. Fischler and R. C. Bolles, "Random sample consensus: A paradigm for model fitting with applications to image analysis and automated cartography," *Commun. ACM*, vol. 24, no. 6, p. 381–395, Jun. 1981.
- [15] S. Ren, K. He, R. Girshick and J. Sun, "Faster R-CNN: towards real-time object detection with region proposal networks," *IEEE Trans. Pattern Analysis and Machine Intelli.*, vol. 39, no. 6, pp. 1137–1149, 1 Jun. 2017.
- [16] K.-L. Low, and A. Ilie. "Computing a view frustum to maximize an object's image area," *J. of Graphics Tools*, vol. 8, no. 15, pp. 1–14, 2003.
- [17] W. Zhang, C. Witharana, W. Li, C. Zhang, X. Li and J. Parent, "Using deep learning to identify utility poles with crossarms and estimate their locations from Google street view images," *Sensors J.*, vol. 18, no. 8, Aug. 2018.

AUTHORS

Mohamed Gaha (gaha.mohamed@hydroquebec.com) received the master's degree in computer science from Université du Québec à Montréal in 2008, and the Ph.D. degree in computer science from École Polytechnique de Montréal, QC, Canada, in 2012. From 2008 to 2012, he was affiliated as a Ph.D. scholar with Hydro-Quebec's Research Institute (IREQ). Since 2012, he works as a full-time researcher at IREQ. His current research interests include asset management, Monte Carlo simulations and machine learning.



Wael Jaafar (waeljaafar@sce.carleton.ca) is an NSERC Postdoctoral Fellow in the Systems and Computer Engineering Department of Carleton University, ON, Canada. He is the recipient of several prestigious grants, such as NSERC Alexandre Graham-Bell (BESC) Canada Graduate Scholarship and the FRQNT (Fonds de recherche du Québec–Nature et technologies) International Internship Scholarship. His current research interests include wireless communications, aerial networks, resource allocation, and machine learning. He is a Senior Member of IEEE.



Jed Fakhfekh (jedfakhfekh@gmail.com) is a software engineer experienced in 3D simulations and computer graphics. He has worked in a wide range of 3D oriented projects, using mainly C++ (std) and Unreal Engine. His current projects focus on 3D tools, engines, and editors LiveLinks.



Guillaume Houle (houle.guillaume2@hydroquebec.com) is a software engineer, graduated from École Polytechnique de Montréal, QC, Canada. He has worked as a research Engineer at the Motor Control Laboratory of McGill University from 2002 to 2012. Since 2012, he works as a full-time researcher at Hydro-Quebec's Research Institute (IREQ). His current research interests include asset management and deep learning for 2D and 3D real world scenes.



Jihene Ben Abderrazak (jihene.benabderrazek@esprit.tn) received the B.Eng. from the Higher School of Communication (SUPCOM), Tunis, Tunisia, in 2006, the M.A.Sc. in Computer Science from the University of Tsukuba, Japan, in 2010 and the Ph.D. degree in Information and Communication Technology from SUPCOM in 2018. She is currently a research assistant at the private school of engineering ESPRIT and is leading the wireless communication research team. Her current research interests include future wireless networks, smart agriculture, autonomous vehicles and machine learning.



Michel Bourgeois (bourgeois.michel@hydroquebec.com) received a B.eng from École de Technologie Supérieure (ETS), Montreal, Canada in 1994. He had worked for more than 15 years in the maintenance industry at Kruger and Pratt and Whitney. Since 2009, he works as a Data analyst at Hydro Quebec. He is currently working on asset management, outage analysis and extreme weather conditions.